Published in final edited form as:
J Phys Chem A. 2012 June 7; 116(22): 5325–5336. doi:10.1021/jp3025705.

Ultrafast Infrared and UV-vis Studies of the Photochemistry of Methoxycarbonylphenyl Azides in Solution

Jiadan Xue[1], **Hoi Ling Luk**[1], **S. V. Eswaran**[2], **Christopher M. Hadad**[1,*], and **Matthew S. Platz**[1,*]

Matthew S. Platz: platz.1@osu.edu

[1]Department of Chemistry, The Ohio State University, 100 West 18th Avenue, Columbus, Ohio, 43210, U.S.A

[2]St. Stephen's College, University of Delhi, Delhi, 110007, India

Abstract

The photochemistry of 4-methoxycarbonylphenyl azide (**2a**), 2-methoxycarbonylphenyl azide (**3a**) and 2-methoxy-6-methoxycarbonylphenyl azide (**4a**) were studied by ultrafast time-resolved infrared (IR) and UV-vis spectroscopies in solution. Singlet nitrenes and ketenimines were observed and characterized for all three azides. Isoxazole species **3g** and **4g** are generated after photolysis of **3a** and **4a**, respectively, in acetonitrile. Triplet nitrene **4e** formation correlated with the decay of singlet nitrene **4b**. The presence of water does not change the chemistry or kinetics of singlet nitrenes **2b** and **3b**, but leads to protonation of **4b** to produce nitrenium ion **4f**. Singlet nitrenes **2b** and **3b** have lifetimes of 2 ns and 400 ps, respectively, in solution at ambient temperature. The singlet nitrene **4b** in acetonitrile has a lifetime of about 800 ps, and reacts with water with a rate constant of 1.9×10^8 $L \cdot mol^{-1} \cdot s^{-1}$ at room temperature. These results indicate that a methoxycarbonyl group at either the *para* or *ortho* positions has little influence on the ISC rate, but that the presence of a 2-methoxy group dramatically accelerates the ISC rate relative to the unsubstituted phenylnitrene. An *ortho* methoxy group highly stabilizes the corresponding nitrenium ion and favors its formation in aqueous solvents. This substituent has little influence on the ring-expansion rate. These results are consistent with theoretical calculations for the various intermediates and their transition states. Cyclization from the nitrene to the azirine intermediate is favored to proceed towards the electron-deficient ester group; however, the higher energy barrier is the ring-opening process, that is azirine to ketenimine formation, rendering the formation of the ester-ketenimine to be less favorable than the isomeric MeO-ketenimine.

Keywords

Ultrafast spectroscopy; photochemistry; aryl azide; arylnitrene

1. Introduction

Arylnitrenes have been extensively studied by nanosecond laser flash photolysis (LFP),[1,2] nanosecond,[3] and picosecond[4] time-resolved Raman spectroscopy (TR[3]), nanosecond time-resolved infrared (TR-IR) and by matrix isolation spectroscopy.[5,6] As a result, a great deal

*Author to whom Correspondence should be addressed. Telephone: 614-688-3141 FAX: 614-292-1685 platz.1@osu.edu, hadad.1@osu.edu.

Supporting Information Available: Ultrafast IR and UV-vis spectra, kinetic data with the fitted curve discussed herein, additional computational data, Cartesian coordinates for the geometries of all species, and full reference of 37 and 38. This material is available free of charge via the Internet at http://pubs.acs.org.

has been learned about their lifetimes and the rate constants of their bimolecular reactions. It is well established that photolysis of aryl azides **1a** in solution usually proceeds by extrusion of molecular nitrogen and the release of a singlet arylnitrene **1b,** that can form a triplet arylnitrene by intersystem crossing (ISC) or generate a ketenimine **1d** through a two-step, ring-expansion reaction through azirine **1c**.[7,8] Certain singlet arylnitrenes can be protonated to form arylnitrenium ions **1f** in the presence of proton donors, such as water or alcohols (Scheme 2). Most arylnitrenes, in solution at ambient temperature, isomerize to form a ketenimine rather than undergo ISC to the ground triplet state, but substituent effects on phenylnitrene chemistry can have a huge influence on the reaction rates of these three processes. For example, a substituent at the para position, especially an electron-donating group can dramatically increase the ISC rate.[9]

Substitution at the *ortho* position has a large impact on the rate of the ring-expansion reaction.[9] A single *ortho* substituent usually has little influence on the rate of singlet phenylnitrene isomerization to the azirine. Singlet 2-methylphenylnitrene, at room temperature has a 1 ns lifetime,[1] the same as that of the parent singlet phenylnitrene. The 2-methyl group directs cyclization to benzazirine away from the substituent for steric reasons. Singlet 2-cyanophenylnitrene[10,11] and 2-acetylphenylnitrene[12] bear sterically undemanding *ortho* substituents. In these two systems, ring-expansion products are formed both by cyclization away from, and towards the substituent.

A di-*ortho* substituent pattern can exert a dramatic steric effect on azirine formation and prolongs the lifetime of the singlet nitrene. Singlet 2,6-dimethylphenylnitrene, for example, has a lifetime of 13 ns.[1]

The electronegativity of *ortho*-substituent(s) can also have a large effect on the lifetimes of singlet nitrenes. A single *ortho*-fluoro substituent(s) increases the barrier for ring expansion by ~1–3 kcal/mol relative to the unsubstituted system,[13,14] thus the singlet 2-fluorophenylnitrene has a lifetime of 8 ns.[13] Fluorine substituents at both *ortho* positions extend the lifetime of singlet 2,6-difluorophenylnitrene to 240 ns.[13,15] Theory has shown that the electron-withdrawing fluorine substituent makes the adjacent carbon very positively charged, and the positive-positive charge interaction between the *ortho* carbon and the carbon bearing nitrogen increases the activation barrier from nitrene to azirine.

Phenylnitrenes with functional groups at the *ortho* position can interact to produce a class of azacyclic compounds[16], such as 2-biphenyl azide which produces carbazole in excellent yield.[17] Upon photolysis of the 2-methoxycarbonylphenyl azide in a matrix at 10 K, Tomioka *et al.*[18] observed *N*-methoxyacetinone **3h** with a carbonyl stretch at 1857 cm^{-1}, and this acetinone **3h** can be photochemically converted to iminoketenes with the observed C=C=O stretches at 2118 and 2088 cm^{-1}.

To our knowledge, there have not been many previous studies of phenylnitrenes substituted with *ortho* ester groups. As azido esters are widely used as polyfunctional reagents for labeling applications, we sought to learn how this substituent influences the ISC rate of the singlet nitrene, and how the steric and substitution combination would affect the rates for ring expansion or ketenimine formation.

Ultrafast time-resolved UV-vis and infrared spectroscopies are effective methods for the study of excited states and reactive intermediates with short lifetimes. They have been utilized to directly characterize the excited states of aryl azides,[19] and some short-lived singlet and triplet nitrenes,[20] ketenimines,[21] and arylnitrenium ions.[5] In this study, we applied ultrafast UV-vis and infrared absorption spectroscopies to study the photochemistry of 4-methoxycarbonylphenyl azide **2a**, 2-methoxycarbonylphenyl azide **3a** and 2-

methoxy-6-methoxycarbonylphenyl azide **4a** in organic and aqueous solutions at room temperature. The carbonyl group imparts reactive intermediates with strong IR vibrations so that one can hope to directly observe and identify singlet and triplet nitrenes, ketenimine, and isoxazole species as well as the corresponding nitrenium ions, while also monitoring their formation rates or lifetimes in different solvents.

2. Experimental and Computational Methods

2.1 Synthesis

2-, 4-methoxycarbonylphenyl azide were synthesized from the corresponding commercially available amines according to the standard method of Tomioka.[22]

2-Methoxy-6-methoxycarbonylphenyl azide—To a solution of 1.00 g (5.98 mmol) of 2-amino-3-methoxybenzoic acid in 25 mL of methanol was added 5 mL of concentrated sulfuric acid. The reaction mixture was heated under reflux for 40 h. The cooled reaction mixture was added with sodium bicarbonate solution until the effervescence ceased. The organic material was extracted with dichloromethane (2 × 100 mL) and washed with brine (50 mL) and water (50 mL). The extract was dried over anhydrous $MgSO_4$, filtered, and the solvent was removed under reduced pressure to give 1.0 g (92 %) 2-methoxy-6-methoxycarbonylphenylamine as a yellowish brown liquid. To a solution of 1.00 g (5.52 mmol) of 2-methoxy-6-methoxycarbonylphenylamine in 12 mL of tetrahydrofuran was added a mixture of concentrated hydrochloric acid (3 mL) and water (24 mL). The reaction mixture was stirred for 15 min in an ice-methanol bath, and a solution of 609 mg (8.83 mmol) of $NaNO_2$ in 10 mL of water was added dropwise to the solution, keeping the temperature of the reaction below 5 °C. The reaction mixture was stirred for 15 min at 0 °C and excess nitrous acid was removed by the addition of urea. To the cooled reaction mixture was added dropwise a solution of 857 mg (8.83 mmol) of NaN_3 in 11 mL of water. After the addition was complete, the reaction mixture was stirred for 1 h at room temperature. The organic material was extracted with dichloromethane and the extract was washed with dilute hydrochloric acid (0.1 M) and dried over anhydrous Na_2SO_4. The solvent was removed under reduced pressure to give an orange crude product. The residue was developed on a silica gel column with 2:5:9 (dichloromethane: ethyl acetate: hexane) give 762 mg (67 %) of 2-methoxy-6-methoxycarbonylphenylazide as yellow liquid (frozen to solid in refrigerator): ^{1}H NMR (400 MHz, $CDCl_3$) δ 3.94 (s, 3H), 3.92 (s, 3H) 7.04 (dd, J = 1, J = 8, 1H), 7.13 (t, J = 8, 1H), 7.36 (dd, J = 2, J = 8, 1H). ^{13}C NMR (400 MHz, $CDCl_3$) δ 168.7, 147.1, 141.8, 122.5, 114.6, 112.9, 110.1, 55.72, 51.5. HRMS (ESI) *m/z* calcd for $C_9H_9N_3O_3$ ($M\text{-}Na^+$) 207.0644, found 207.0612.

2.2 Ultrafast Spectroscopy

The ultrafast UV-vis broadband and ultrafast infrared absorptions measurements were performed using the home-built spectrometers at The Ohio State University for Chemical and Biophysical Dynamics. These instruments have been described in detail elsewhere.[19,23]

The sample solutions were prepared to provide absorption at the excitation wavelength to be ~1 (0.5 and 1 mm spacers for ultrafast IR and UV-vis experiments, respectively).

2.3 Computational Methods

Geometry optimizations and transition state searches were performed using the 6-31+G(d,p)[24,25] basis set in conjunction with the B3LYP[26,27] method or the 6-31G* [28] basis set in conjunction with the complete active space self-consistent field (CASSCF) method.[29,30] The CASSCF calculations used an 10-electron, 10-orbital active space, hereafter designated (10,10) for all species. The ten orbitals comprised of the eight orbitals

included in the active space, and these are analogous to those used in similar calculations on species involved in the ring expansion of phenylnitrenes,[31] along with the bonding and antibonding orbitals (π, π^*) of the C=O bond in the ester group. The nature of all stationary points, either minima or transition states, was determined by calculating the vibrational frequencies at either the B3LYP/6-31+G(d,p) or CASSCF(10,10)/6-31G* level. The unscaled frequencies were used to obtain corrections for zero-point vibrational energies. For DFT calculations, we have employed unrestricted B3LYP methods and found broken-symmetry solutions for the open-shell singlet nitrenes and the corresponding transition states for azirine formation, as has been described in the literature.[32] The effects of dynamic electron correlation[33] were determined by CASPT2 calculations[34,35] using either 6-31G* or Dunning's correlation-consistent polarized valence double-zeta basis set (cc-pVDZ),[36] while using the CASSCF(10,10)/6-31G* optimized geometries. All calculations were performed using the Gaussian 09[37] and MOLCAS version 7.4[38] software packages.

3. Results and Discussion

3.1 Ultrafast Time-Resolved Infrared Spectroscopic Results for 4-Methoxycarbonylphenyl Azide

Ultrafast laser flash photolysis (LFP) of 4-methoxycarbonylphenyl azide **2a** in acetonitrile (MeCN) with 270 nm light produces the transient IR spectra in the 1920–1830 cm^{-1} region shown in Figure 1. The band observed is easily recognized as a 1,2-didehydroazepine (ketenimine) absorption.[39–41a] Inspection of Figure 1 shows that the initially detected vibrational band is broad, then sharpens and blue-shifts over initial 30 ps. This is consistent with previous reports that hot singlet nitrenes can isomerize to hot benzazirines and then to the thermally excited ketenimines which then undergo vibrational relaxation.[21] There are only a few direct observations of benzairines[41b,c] because their barrier to ring opening is rather small,[31,41d] The kinetics of the ketenimine formation was monitored at 1888 cm^{-1} and the decay was fit with a bi-exponential function, yielding time constants of ~15 ps (41%) and ~2200 ps (59%). These values correspond to the vibrational cooling (VC)[19,20,42–45] of hot ketenimine formed in the reaction of hot singlet nitrene and to formation of the ketenimine via relaxed singlet nitrene/benzazirine, respectively.

Figure 2 presents transient IR spectra in the 1780–1660 cm^{-1} region obtained under the same conditions as those of Figure 1. A broad band with a maximum at 1697 cm^{-1} was detected immediately after the laser pulse, shown as the spectrum obtained at 0.7 ps delay time, and this band narrows and its intensity increases slightly within 3 ps of the laser pulse (Figure 2A). Then, this 1697 cm^{-1} band blue-shifts to 1701 cm^{-1} over 17 ps. Finally, the 1701 cm^{-1} band decays with a time constant of ~2000 ps to give a new band at 1714 cm^{-1} with a clear isosbestic point at 1708 cm^{-1}, shown in Figure 2C. The 1697–1701 cm^{-1} band is the carbonyl stretch of the hot and the thermally relaxed singlet nitrene **2b**, and the band narrowing and blue shift can be attributed to a mixture of VC, solvent reorganization[46] and ring expansion of the hot singlet nitrene. The new band, with a maximum at 1714 cm^{-1}, partly overlaps with the bleaching of the carbonyl band of the ground state azide. This effect artificially distorts the appearance of the 1722 cm^{-1} bleaching to appear (incorrectly) as a recovery at post delay times. The 1714 cm^{-1} positive band observed in Figure 2C is the ester carbonyl stretch of the ketenimine, and its formation can be fitted with the same time constant as the carrier of the characteristic C=C=N stretching at 1888 cm^{-1} displayed in Figure 1. Although density functional theory (DFT, B3LYP) calculations predict that the singlet nitrene (**2b**), triplet nitrene (**2e**) and ketenimine (**2d**) have rather similar carbonyl stretching frequencies, there is no evidence for the formation of a second species formed as the singlet nitrene is decaying. To our knowledge, this is the first direct observation of a singlet arylnitrene using time-resolved infrared spectroscopy.

Analogous ultrafast time-resolved infrared experiments were performed with the 4-methoxycarbonylphenyl azide **2a** in MeCN:D_2O (1:1) mixed aqueous solvent, and the spectra are presented in the Supporting Information. The ultrafast infrared experimental results demonstrate that the presence of water has no influence on the chemistry and the kinetics of singlet nitrene **2b**.

3.2 Ultrafast Time-Resolved Infrared Spectroscopic Results for 2-Methoxycarbonylphenyl Azide

Ultrafast LFP of 2-methoxycarbonylphenyl azide **3a** with 270 nm excitation in neat MeCN and in MeCN:D_2O (2:1) mixed aqueous solvent generates ketenimine **3d** with a time constant of ~400 ps in each solvent system. The transient infrared spectra recorded in the 1920–1830 cm^{-1} region and the associated kinetic information is presented in the Supporting Information. As with azide **2a**, the IR spectrum of photo-generated ketenimine **3d** shows a characteristic C=C=N stretching band at 1883 cm^{-1}, and the kinetics can be fit to a bi-exponential function, reflecting the VC of hot ketenimine and formation of the ketenimine via relaxed singlet nitrene/benzazirine, respectively.

Figure 3 displays the ultrafast IR spectra recorded in the 1770–1670 cm^{-1} region upon 270 nm excitation of 2-methoxycarbonylphenyl azide **3a** in MeCN. The IR spectra obtained in the MeCN:D_2O (2:1) mixed aqueous solvent are presented in the Supporting Information. The hot singlet nitrene **3b** is generated immediately after the laser pulse as depicted in the transient absorption spectrum recorded 0.7 ps after the laser pulse. The hot singlet nitrene then undergoes VC to form the relaxed singlet nitrene **3b**, and both species contribute to the generation of a new carbonyl vibrational band at 1715 cm^{-1} as displayed in Figure 3B at various post-excitation delays. The kinetics of the new band formation were monitored at 1715 cm^{-1} and fit using a bi-exponential function with time constants of ~9 ps (52%) and ~ 430 ps (48%). By analogy to the transient IR spectra observed in the same region after LFP photolysis of the azide **2a**, the growing 1715 cm^{-1} band in Figure 3B is assigned to the ketenimine. This result is in agreement with the spectra of hot and relaxed ketenimine obtained in the 1880 cm^{-1} region. We expect both ketenimine isomers to be formed based on calculations to be discussed later.

In addition to ketenimine, a second new species is formed near 1640 cm^{-1} as shown in Figure 4. The carrier of this signal has a lifetime of more than 3 ns. Examination of Figure 4 shows that this new species was generated in a very hot state immediately after the laser pulse, and that the new species is largely produced from the hot singlet nitrene. The new band at 1640 cm^{-1} was observed only upon LFP of 2-methoxycarbonylphenyl azide **3a** and 2-methoxy-6-methoxycarbonylphenyl azide **4a** *(vide infra),* but not with 4-methoxycarbonylphenyl azide **2a**. This leads us to conclude that the new species absorbing at 1640 cm^{-1} is isoxazole **3g** (Scheme 3). By applying a scaling factor[47] of 0.9648, our DFT calculations predict that this isoxazole type species **3g** has a scaled IR frequency at 1631 cm^{-1}, corresponding to the C=C stretching mode in the 5-membered ring, with a strong intensity (see Supporting Information for details). This prediction is in excellent agreement with the experimental IR result. The new species **3g** was also observed in the MeCN:D_2O (2:1) mixed aqueous solvent with the same formation kinetics as that observed in neat MeCN.

3.3 Ultrafast Time-Resolved Infrared Spectroscopic Results for 2-Methoxy-6-methoxycarbonylphenyl Azide

Ultrafast LFP of 2-methoxy-6-methoxycarbonylphenyl azide **4a** in MeCN with 272 nm excitation in neat MeCN produces the isoxazole **4g** and the ketenimine **4d**. The transient infrared spectra and kinetic information are presented in the Supporting Information. As was

found with 2-methoxycarbonylphenyl azide, an isoxazole species **4g** is formed as evidenced by a band at 1645 cm^{-1}. In order to confirm the presence of isoxazole, steady state infrared spectra were recorded before and after photolysis (Figure 5S). The growth of the absorption at 1632 cm^{-1} after photolysis further supports the formation of isoxazole species **4g**.

The ketenimine has a characteristic C=C=N stretching band at 1880 cm^{-1}, and its formation kinetics can be fit with a bi-exponential function reflecting the VC of the hot ketenimine (~12 ps, 54%) and formation of the ketenimine via relaxed singlet nitrene/benzazirine (~ 800 ps, 46%), respectively. The ketenimine has a lifetime of more than 3 ns under these experimental conditions.

The transient IR spectra observed in the 1765–1655 cm^{-1} region after photolysis of azide **4a** in MeCN shows one distinct difference compared to the data obtained with azides **2a** and **3a** in the same solvent. As shown in Figure 5B, a third new band at 1755 cm^{-1}, which is at a higher IR frequency than the azide bleach at 1730 cm^{-1}, is formed with the same time constant (~ 800 ps) as the singlet nitrene **4b** (1700 cm^{-1}) decays. The new species at 1755 cm^{-1} is tentatively assigned to triplet nitrene **4e** rather than the other possible ketenimine isomer or its benzazirine analog, because theory predicts that ring expansion towards the ester group has a very large activation barrier (*vide infra*). This assignment is also in agreement with the DFT predicted (and scaled) IR frequencies of triplet nitrene **4e** (1708 cm^{-1}) as this species was found to have a slightly higher IR frequency than the azide bleach predicted at 1707 cm^{-1} at the same level of theory.

Assuming these assignments are valid we deduce that the singlet nitrene **4b** undergoes both ring expansion and ISC in MeCN, to form the ketenimine and the triplet nitrene, respectively. This interpretation postulates that the 2-methoxy group accelerates the ISC rate relative to unsubstituted singlet phenylnitrene[2], in the same manner as does a *para*-methoxy substituent.[9]

We cannot exclude the possibility that the carrier of the 1755 cm^{-1} band is a benzazirine in an unusually deep minimum as both benzazirine **4c′** and triplet nitrene **4e** give the same predicted carbonyl stretch at 1708 cm^{-1}. We prefer the triplet nitrene as our tentative assignment since observations of benzazirines are quite rare.[41b,c] Moreover, as mentioned previously, it seems reasonable to expect that an *ortho* methoxy group to accelerate ISC in a manner similar to that of a *para* methoxy group[9].

Similar ultrafast IR experiments were performed in MeCN:D_2O (1:1) with azide **4a**, and the spectra recorded in the 1780–1660 cm^{-1} region are shown in Figure 6. The positive band at 1690 cm^{-1}, detected at early delay times (Figure 6A) is assigned to singlet nitrene **4b**, and the absorption band blue-shifts within the initial 15 ps due to VC. While the singlet nitrene band is decaying, a positive band at 1700 cm^{-1} rises and with an isosbestic point at 1704 cm^{-1}. This 1700 cm^{-1} band cannot be assigned to the corresponding ketenimine since the 1880 cm^{-1} band is not generated with this azide (**4a**), in the presence of water, upon laser photolysis. We assign this new species to nitrenium ion **4f** because the nitrenium ion was observed and characterized in the ultrafast UV-vis experiments (see below for details). DFT calculations predicted that the nitrenium ion **4f** has a scaled carbonyl stretching band at 1737 cm^{-1} with a calculated strong intensity. The production of the nitrenium ion accelerates the decay of singlet nitrene **4b**, monitored at 1693 cm^{-1}, and fit to an exponential function with a decay time constant of ~400 ps. Less triplet nitrene **4e** is generated in the presence of water as only a low intensity characteristic band is present at 1755 cm^{-1} in Figure 6B.

3.4 Ultrafast UV-vis Spectroscopic Results with 2-Methoxy-6-methoxycarbonylphenyl Azide

Ultrafast LFP (Λ_{ex}=313 nm) of 2-methoxy-6-methoxycarbonylphenyl azide **4a** in MeCN produces the transient UV-vis spectra shown in Figure 7. The first species detected is observed immediately after the laser pulse, at 460 nm. The absorption maximum blue shifts within 1 ps. This species is attributed to the S_1 state of azide **4a**. This also agrees with the predictions of time-dependent density functional theory (TD-DFT, details below) that 313 nm light excites the azide to its S_1 state. As the S_1 state of azide **4a** decays, a transient absorption spectrum attributed to the singlet nitrene **4b** grows in at 450 nm. Between 1 and 10 ps, after the laser pulse, the transient absorption band of the singlet nitrene grows and narrows due to solvation[48] and VC.[42–45] The relaxed singlet nitrene has a lifetime of 747 ± 100 ps in MeCN consistent with the ~800 ps time constant obtained in ultrafast IR experiment for the singlet nitrene **4b**.

Figure 8 presents the ultrafast time-resolved UV-vis spectra recorded in a MeCN:H_2O (3:1) mixed aqueous solvent system after LFP (Λ_{ex}=313 nm) of azide **4a**. As in MeCN, in the mixed aqueous solvent, the S_1 state of the azide is generated immediately after the laser pulse and decays within 1 ps to produce the singlet nitrene. In contrast to the results obtained in MeCN, the singlet nitrene decay in the mixed solvent produces a new absorption band at 530 nm. The band grows with an isosbestic point at 490 nm and a time constant of 429 ± 54 ps. This transient has a lifetime longer than our instrumental limit (3 ns). Based on McClelland and co-workers studies of *para* substituted phenyl azide by ns LFP,[49–52] the new transient species produced in aqueous solvent is assigned to the singlet nitrenium ion, in good agreement with TD-DFT calculations in water that predict that the nitrenium ion **4f** has maximum absorption at 531 nm.

Similar experiments were performed for the azide in MeCN:H_2O as a mixed aqueous solvent, in different proportions, and the ultrafast UV-vis spectra are shown in the Supporting Information. As the content of water increases from 25% to 50% in solution, the nitrenium ion forms more rapidly with a time constant of ~400 ps in 25% aqueous solution to ~200 ps in 50% aqueous solution. The pseudo first order rate constant of formation of the nitrenium ion was plotted as a function of the water concentration as shown in Figure 10S and well fit to a linear function, so that the first order rate constant for the singlet nitrene **4b** towards water $k_{[H2O]}$ was found to be 1.9×10^8 $L \cdot mol^{-1} \cdot s^{-1}$.

3.5 Ketenimine Assignment and Calculations of the Activation Barrier to Singlet Nitrene Ring Expansion

To aid in understanding the experimental results obtained with these nitrenes and the assignment of the different species observed, we performed a series of calculations on the two-step, ring-expansion reactions for the corresponding nitrenes using both density functional theory (DFT)[26,27] and complete active space self-consistent field (CASSCF)[29,30] with second-order perturbation theory (CASPT2) corrections.[34,35] These results provide an overall view of the energetics of the ring expansion process for methoxycarbonylarylnitrenes. We remind the reader that singlet phenylnitrene has a preferred open-shell configuration, and CASSCF methods, while challenging for determining the ideal or most practical active space, provide greater confidence for an accurate description of the open-shell nitrene.

For singlet 4-methoxycarbonylphenylnitrene **2b** at the CASPT2/cc-pVDZ//CASSCF(10,10)/6-31G* level of theory (Figure 9), we found an activation barrier of 7.5 kcal/mol to form the ketenimine which is comparable to that of unsubstituted phenylnitrene. However, for singlet 2-methoxycarbonylphenylnitrene **3b** (Figure 10), the activation barrier for cyclization to

form the azirine is much smaller (2 – 3 kcal/mol). A possible reason for this result is the decreased stability of the singlet *ortho*-methoxycarbonylphenylnitrene **3b** relative to that of *para* singlet nitrene **2b**. For both singlet nitrenes, the carbonyl group prefers to be in plane with the phenyl ring to achieve higher conjugation and stability. However, when the carbonyl group is in the *ortho* position, this results in severe repulsion between the nitrene nitrogen and the carbonyl oxygen. Hence, it is found that the CASPT2 energy for *ortho* singlet nitrene **3b** is 4.5 kcal/mol higher than that of *para* **2b**. This increase in energy of the singlet nitrene decreases the activation energy barrier to cyclization to form azirine. This also explains why the cyclization of **3b** to form azirine **3c** is much faster than the unsubstituted singlet nitrene **1b** as moving the nitrene nitrogen out of plane relieves steric repulsion through cyclization.

From the CASPT2 results, it is likely that both isomeric ketenimines are formed from the *ortho* methoxycarbonyl substituted singlet phenylnitrene. Unfortunately, IR spectroscopy cannot distinguish between these two ketenimines by either vibrational frequency or kinetics, due to their very similar infrared vibrations (less than 20 cm^{-1} difference). The energy barriers to formation of the two isomers are predicted to be similar; thus, their rates of formation are expected to be similar.

Let us now discuss the potential energy surface for 2-methoxy-6-methoxycarbonylphenylnitrene, **4b**, which has two *ortho* substituents: a methoxy and a methoxycarbonyl moiety on phenylnitrene. For the singlet nitrene **4b**, the ring-expansion reaction can proceed either towards or away from the ester group, and produce two ketenimine isomers as shown in Figure 11. (In Figure 13S, we also present the relative energy profiles obtained from B3LYP/6-31+G(d,p) and CASPT2(10,10)/6-31G*//B3LYP/6-31+G(d,p) calculations. Additional figures and computational details are provided in the Supporting Information.) The CASPT2/6-31G*//CASSCF(10,10)/6-31G* calculations predict that the ester-ketenimine is less stable than the MeO-ketenimine and the latter is 9.9 kcal/mol lower in energy than the ester-ketenimine. Similar to the case of 2-methoxycarbonylphenylnitrene **2b**, the activation barrier is small for the cyclization step. However, the barrier for ring-opening to form ester-ketenimine is extremely high (13.5 kcal/mol). This would lead us to the conclusion that MeO-ketenimine **4d** would be the only possible ketenimine formed at room temperature. In order to confirm the accuracy of the potential energy surface's topology, CASPT2 single-point energy calculations were performed on the B3LYP/6-31+G(d,p) optimized geometries, and these results are shown in Figure 13S. The CASPT2 calculations are consistent with each other and independent of a B3LYP or CASSCF geometry. The different topology observed with the B3LYP energies can be attributed to spin contamination of the singlet (open-shell) nitrene and the transition states for azirine formation. We did attempt CASPT2 calculations with the cc-pVDZ basis set, as described earlier for 2-methoxycarbonyl and 4-methoxycarbonylphenylnitrene; however, those attempts failed due to challenges in defining the correct active spaces for the singlet nitrene and the transition states for azirine formation. Nevertheless, since the azirines, the ketenimines, and their transition states are well described by a closed-shell description, we also used higher level CBS-QB3[53] calculations (see Supporting Information, Table 34S) to provide accurate values for the conversion of azirine to ketenimine. At the CBS-QB3 level of theory, the activation barrier for conversion of the ester-azirine to the ester-ketenimine is large (9.1 kcal/mol), while the corresponding barrier is only 0.4 kcal/mol to go from the MeO-azirine to the MeO-ketenimine. These results are consistent across the various levels of theory: B3LYP (9.0 vs 1.3 kcal/mol), CASPT2//CASSCF (13.5 vs 2.2 kcal/mol) and CASPT2//B3LYP (12.1 vs 2.5 kcal/mol), respectively.

Usually, cyclization of a phenylnitrene to a benzazirine is much slower than subsequent ring-opening of the benzazirine to ketenimine. However, the increase in energy of the singlet

nitrene changes the topology of the potential energy surface describing the formation of ketenimine. In the *ortho* substituted system, cyclization to form azirine is no longer the rate-determining step; instead, azirine formation by insertion towards the methoxy group leads to subsequent ring-expansion and ketenimine formation (**4d**) as the preferred kinetic and thermodynamic product.

B3LYP predictions of the IR frequencies are in good agreement with the assignment of the ketenimine species **4d** observed in the ultrafast IR spectrum displayed in Table 1. The calculation of MeO-ketenimine **4d** shows that this species has strong infrared vibrations at 1866 and 1705 cm^{-1}, and this result is consistent with the experimentally observed ultrafast IR spectra in which two positive vibration bands were observed at 1880 and 1716 cm^{-1}.

The calculations predict that benzazirine **4c′** is the kinetic product and exists in a relatively deep energy minimum. Thus it is possible that this species is the carrier of the 1755 cm^{-1} band, and not the triplet nitrene. Given that we are decomposing the azide precursor with 270 nm light, we expect and observe that singlet nitrene **4b** is formed with substantial excess vibrational energy. Thus, we hypothesize that **4b** has sufficient energy to explore the potential energy surface and find a pathway to the thermodynamic, singlet state product ketenimine **4d**. Thus, we tentatively assign the carrier of 1755 cm^{-1} band to the global minimum, the triplet nitrene. We also prefer this assignment because of the expectation that an *ortho* methoxy substituent will accelerate ISC in the same manner as a para methoxy group[9].

3.6 The Influence of Ester and Methoxy Substituents on the Singlet Nitrene

Distinct from a single *ortho* or *para* methyl or fluorine substituent, which have similar effects on the ring-expansion rate of a singlet phenyl nitrene, the ester group has a very different influence on the ring expansion of the singlet nitrenes depending on whether it is positioned at the *para* or *ortho* position. For example, singlet 4-methoxycarbonylphenylnitrene **2b** forms the ketenimine with a time constant of 2200 ps, while we observe a 400 ps time constant for the 2-methoxycarbonyl analog. These experimental results are consistent with the predictions of theory. CASPT2 calculations predict that the activation barrier to form ketenimine is 7.5 kcal/mol and 2–3 kcal/mol for 4-methoxycarbonyl- and 2-methoxycarbonylphenylnitrenes, respectively. This difference can be attributed to the greater ability of the carbonyl group to localize the electron in the non-bonding **π** orbital at the *ortho* carbon to which the substituent is attached. This explanation has been proposed previously by Gritsan and coworkers[11] following study of the 2-, 3- and 4- cyano-substituted singlet phenylnitrenes. In that study, the 4-cyano phenylnitrene was found to have a slower cyclization rate than the 2-cyano phenylnitrene. The cyclization at a substituted 2-carbon is much faster when the substituent is cyano, rather than methyl or fluoro.[11]

The ultrafast IR and UV-vis experimental results show that the lifetime of relaxed 2-methoxy-6-methoxycarbonylphenyl singlet nitrene **4b** is ~800 ps in MeCN at room temperature. This lifetime is similar to that of the parent singlet phenylnitrene, ~1 ns, in solution at room temperature but the parent lifetime is controlled by benzazirine formation and not ISC, which has a rate constant (determined at low temperature) of ~ 10^6 s^{-1}.[2] Based on our spectroscopic assignments we posit that both the triplet nitrene and the ketenimine are form while the relaxed singlet nitrene **4b** decays. In this interpretation, the ISC rate for **4b** must be much faster than the ISC rate of parent phenylnitrene (3.2×10^6 s^{-1}),[2] determined at low temperature, and comparable to that found previously with 4-methoxyphenylnitrene, which was estimated to be greater than 5×10^8 s^{-1} by laser flash photolysis measurements.[9] We propose that the 2-methoxy group promotes a large acceleration of the ISC rate as it

increases the zwitterionic character of the singlet nitrene relative to the parent system, which facilitates a spin-orbit coupling mechanism of ISC.[54]

Ketenimine formation rate was estimated to be $(0.1–1.2)\times10^9$ s^{-1}, which is similar to that of parent and 2-methyl and di-*ortho* methyl substituted analogues, but faster than the di-*ortho* fluoro substituted phenylnitrene.[13] The fast formation rate of ketenimine deduced from ultrafast IR experiments indicates that the di-*ortho* substituent pattern examined here has little influence on the rate of ketenimine formation. However, the ester group has a large directing effect on cyclization that is steric in nature. Ring expansion for the singlet 2-methoxy-6-methoxycarbonylphenylnitrene greatly prefers cyclization towards the methoxy group rather than the ester group.

The ultrafast IR data and the theoretical calculations results demonstrate that MeO-ketenimine is more stable and formed more rapidly than the ester-ketenimine. However, our CASPT2 calculations (Figure 11) showed that cyclization to benzazirine is faster towards the electron-deficient ester group, and these theoretical results are consistent with the previous cyano-substituted singlet phenylnitrene study[11] by Gritsan *et al.* However, in our case, the calculated higher energy barrier in the second step of ring-opening, that is azirine to ketenimine formation, renders the formation of the ester-ketenimine to be unfavorable. Hence, we predict that the MeO-ketenimine (**4d**) is formed in preference to the ester-ketenimine (**4d′**) and interpret the time resolved data accordingly.

3.7 The Photochemistry of 2-Methoxycarbonylphenyl Azide and the Formation of Isoxazole

Tomioka[18] and coworkers did not observe the formation of isoxazole **3g** in their low temperature, matrix-isolation spectroscopy study of the photochemistry of 2-methoxycarbonylphenyl azide. The observation of the 1640 cm^{-1} band, however, by ultrafast time-resolved IR spectroscopy in this paper provides evidence for the formation of the isoxazole **3g**. Another reason for the assignment of 1640 cm^{-1} IR band to isoxazole **3g** rather than azetinone **3h** is that the 1857 cm^{-1} (C=O stretching in **3h**[18]) IR band was not observed upon 270 nm laser pulse photolysis of azide **3a** in MeCN and in mixed aqueous solution. Moreover, there was no evidence for the existence of imino ketenes species formation by photointerconversion from azetinone[18] in our fs time resolved IR experiments on photolysis of azide **4a** in MeCN.

The absence of detection of azetinone **3h** is in agreement with the results of Sun *et al.*[55] This group, using nano-second IR spectroscopy, detected ketenimine as the only intermediate (on the microsecond time scale) in *n*-heptane at room temperature. Thus, we conclude that at room temperature, the singlet nitrene **3b** decays by producing the ketenimines **3d** (**3d′**) and isoxazole **3g**, respectively.

From calculations, we predict that there is an activation barrier of 10.5 kcal/mol (CASPT2/cc-pVDZ//CASSCF(10,10)/6-31G*) to form the isoxazoles. This large activation barrier explains why we only observe the formation of the isoxazole from vibrationally hot singlet nitrenes while only ketenimines are formed from the vibrationally relaxed singlet nitrene.

In contrast to the CASPT2 calculations, DFT calculations predict a much lower activation energy barrier (2.7 kcal/mol) to isoxazole formation. The discrepancy can be attributed to the failure to accurately consider the open-shell nature of the singlet nitrene. The related isoxazole can be formed from **4b** with an activation barrier of 9.3 kcal/mol (CASPT2/cc-pVDZ//CASSCF(10,10)/6-31G*).

4. Conclusions

As shown in Scheme 3, 270 nm laser photolysis of 4-, 2-methoxycarbonylphenyl and 2-methoxy-6-methoxycarbonylphenyl azides generate singlet nitrenes from initial excitation to the azide S_n (n > 1) excited state. The initially formed singlet nitrenes are born vibrationally excited. Singlet nitrene **2b** has a lifetime of 2 ns in MeCN and in mixed aqueous solvent at room temperature. Singlet nitrene **3b** produces the ketenimine and isoxazole **3g**, with a time constant of 400 ps in solution. Singlet nitrene **4b**, in MeCN, produces ketenimine by ring expansion towards the methoxy group and isoxazole **4g** by reaction with the carbonyl oxygen. Based on DFT calculations and the behavior of 4-methoxy phenyl nitrene[9], we propose singlet nitrene **4b** rapidly forms triplet nitrene **4e** as well. These results demonstrate that the methoxycarbonyl group at both the *para* and *ortho* positions have little influence on the ISC rate. In water containing solvent systems, most of the singlet nitrene **4b** formed in solution is protonated to produce nitrenium ion **4f**. The ortho methoxy group stabilizes the nitrenium ion and accelerates its formation in the presence of water, but has little influence on the ring-expansion rate.

Supplementary Material

Refer to Web version on PubMed Central for supplementary material.

Acknowledgments

The ultrafast experiments were performed at the Ohio State Center for Chemical and Biophysical Dynamics, established with the generous support of the National Science Foundation. Support of this work by the National institutes of Health (R01-GM073666) is gratefully acknowledged.

References

1. Gritsan NP, Gudmundsdottir AD, Tigelaar D, Platz MS. J Phys Chem A. 1999; 103:3458–3461.
2. Gritsan NP, Zhu Z, Hadad CM, Platz MS. J Am Chem Soc. 1999; 121:1202–1207.
3. Xue J, Du Y, Chuang YP, Phillips DL, Wang J, Luk HL, Hadad CM, Platz MS. J Phys Chem A. 2008; 112:1502–1510. [PubMed: 18225870]
4. Kwok WM, Chan PY, Phillips DL. J Phys Chem B. 2004; 108:19068–19075.
5. Wang J, Burdzinski G, Zhu Z, Platz MS, Carra C, Bally T. J Am Chem Soc. 2007; 129:8380–8388. [PubMed: 17567009]
6. Morawietz J, Sander W. J Org Chem. 1996; 61:4351–4354. [PubMed: 11667336]
7. Lwowski, W. Nitrenes. Wiley; New York, N.Y: 1970.
8. Scriven, EFV. Azides and Nitrenes. Academic Press; New York, N.Y: 1984.
9. (a) Gritsan NP, Tigelaar D, Platz MS. J Phys Chem A. 1999; 103:4465–4469.(b) Gritsan, NP.; Platz, MS. Photochemistry of azides : the azide/nitrene interface. In: Bräse, S.; Banert, K., editors. Organic Azides: Syntheses and Applications. John Wiley & Sons, Ltd; West Sussex, UK: 2010. p. 311-364.
10. Lamara K, Redhouse AD, Smalley RK, Thompson JR. Tetrahedron. 1994; 50:5515–5526.
11. Gritsan NP, Likhotvorik I, Tsao ML, Celebi N, Platz MS, Karney WL, Kemnitz CR, Borden WT. J Am Chem Soc. 2001; 123:1425–1433.
12. Berwick MA. J Am Chem Soc. 1971; 93:5780–5786.
13. Gritsan NP, Gudmundsdottir AD, Tigelaar D, Zhu Z, Kahley MJ, Hadad CM, Platz MS. J Am Chem Soc. 2001; 123:1951–1962. [PubMed: 11456816]
14. Karney WL, Borden WJ. J Am Chem Soc. 1997; 119:3347–3350.
15. Mandel S, Liu J, Hadad CM, Platz MS. J Phys Chem A. 2005; 109:2816–2821. [PubMed: 16833595]
16. Wentrup C. Adv Heterocycl Chem. 1981; 28:231–361.

17. Smith PAS, Brown BB. J Am Chem Soc. 1951; 73:2435–2437.
18. Tomioka H, Ichikawa N, Komatsu K. J Am Chem Soc. 1993; 115:8621–8626.
19. Burdzinski G, Hackett JC, Wang J, Gustafson TL, Hadad CM, Platz MS. J Am Chem Soc. 2006; 128:13402–13411. [PubMed: 17031952]
20. Wang J, Kubicki J, Burdzinski G, Hackett JC, Gustafson TL, Hadad CM, Platz MS. J Org Chem. 2007; 72:7581–7586. [PubMed: 17824713]
21. Burdzinski G, Middleton CT, Gustafson TL, Platz MS. J Am Chem Soc. 2006; 128:14804–14805. [PubMed: 17105280]
22. Murata S, Abe S, Tomioka H. J Org Chem. 1997; 62:3055–3061. [PubMed: 11671685]
23. Wang J, Burdzinski G, Platz MS. J Am Chem Soc. 2008; 130:11195–11209. [PubMed: 18656918]
24. Clark T, Chandrasekhar J, Spitznagel GW, Schleyer PvR. J Comput Chem. 1983; 4:294–301.
25. Frisch MJ, Pople JA, Binkley JS. J Chem Phys. 1984; 80:3265–3269.
26. Becke AD. J Chem Phys. 1993; 98:5648–5652.
27. Lee C, Yang W, Parr RG. Phys Rev B. 1988; 37:785–789.
28. Hariharan PC, Pople JA. Theor Chim Acta. 1973; 28:213–222.
29. Roos BO. Adv Chem Phys. 1987; 69:339–445.
30. Roos BO. Int J Quantum Chem Symp. 1980; 14:175–189.
31. Karney WL, Borden WT. J Am Chem Soc. 1997; 119:1378–1387.
32. Johnson WTG, Sullivan MB, Cramer CJ. Int J Quant Chem. 2001; 85:492–508.
33. Moller C, Plesset MS. Phys Rev. 1934; 46:618–622.
34. Andersson K, Malmqvist PA, Roos BO, Sadlej AJ, Wolinski K. J Phys Chem. 1990; 94:5483–5488.
35. Andersson K, Malmqvist PA, Roos BO. J Chem Phys. 1992; 96:1218–1226.
36. Dunning TH Jr. J Chem Phys. 1989; 90:1007–1023.
37. Frisch, MJ.; Trucks, GW.; Schlegel, HB.; Scuseria, GE.; Robb, MA.; Cheeseman, JR.; Scalmani, G.; Barone, V.; Mennucci, B.; Petersson, GA., et al. Gaussian 09, Revision A.1. Gaussian, Inc; Wallingford CT: 2009.
38. Karlström G, Lindh R, Malmqvist P-Å, Roos BO, Ryde U, Veryazov V, Widmark PO, Cossi M, Schimmelpfennig B, Neogrady P, et al. Computational Materials Science. 2003; 28:222–239.
39. Chapman OL, Le Roux JP. J Am Chem Soc. 1978; 100:282–285.
40. Shields CJ, Chrisope DR, Schuster GB, Dixon AJ, Poliakoff M, Turner JJ. J Am Chem Soc. 1987; 109:4723–4726.
41. (a) Li YZ, Kirby JP, George MW, Poliakoff M, Schuster GB. J Am Chem Soc. 1988; 110:8092–8098.(b) Tsao ML, Platz MS. J Phys Chem A. 2004; 108:1169–1176.(c) Tsao ML, Platz MS. J Am Chem Soc. 2003; 125:12014–12025. [PubMed: 14505423] (d) Gritsan NP, Platz MS. Chem Rev. 2006; 106:3844–3867. [PubMed: 16967923]
42. Wang J, Burdzinski G, Gustafson TL, Platz MS. J Org Chem. 2006; 71:6221–6228. [PubMed: 16872208]
43. Wang J, Burdzinski G, Gustafson TL, Platz MS. J Am Chem Soc. 2007; 129:2597–2606. [PubMed: 17290992]
44. Wang J, Kubicki J, Hilinski EF, Mecklenburg SL, Gustafson TL, Platz MS. J Am Chem Soc. 2007; 129:13683–13690. [PubMed: 17935331]
45. Wang J, Burdzinski G, Platz MS. Org Lett. 2007; 9:5211–5214. [PubMed: 18001041]
46. Nibbering ETJ, Elsaesser T. Appl Phys B. 2000; 71:439–441.
47. Merrick JP, Moran D, Radom L. J Phys Chem A. 2007; 111:11683–11700. [PubMed: 17948971]
48. Wang J, Kubicki J, Gustafson TL, Platz MS. J Am Chem Soc. 2008; 130:2304–2313. [PubMed: 18215044]
49. McClelland RA, Davidse PA, Hadzialic G. J Am Chem Soc. 1995; 117:4173–4174.
50. McClelland RA. Tetrahedron. 1996; 52:6823–6858.
51. McClelland RA, Kahley MJ, Davidse PA, Hadzialic G. J Am Chem Soc. 1996; 118:4794–4803.
52. Davidse PA, Kahley MJ, McClelland RA. J Am Chem Soc. 1994; 116:4513–4514.

53. Montgomery JA, Frisch MJ, Ochterski JW, Petersson GA. J Chem Phys. 2000; 112:6532–6542.
54. Platz, MS. Reactive Intermediate Chemistry. Moss, RA.; Platz, MS.; Maitland Jones, J., editors. John Wiley & sons, Inc; Hoboken, New Jersey: 2004. p. 501-559.
55. Sun XZ, Virrels IG, George MW, Tomioka H. Chem Lett. 1996:1089–1090.

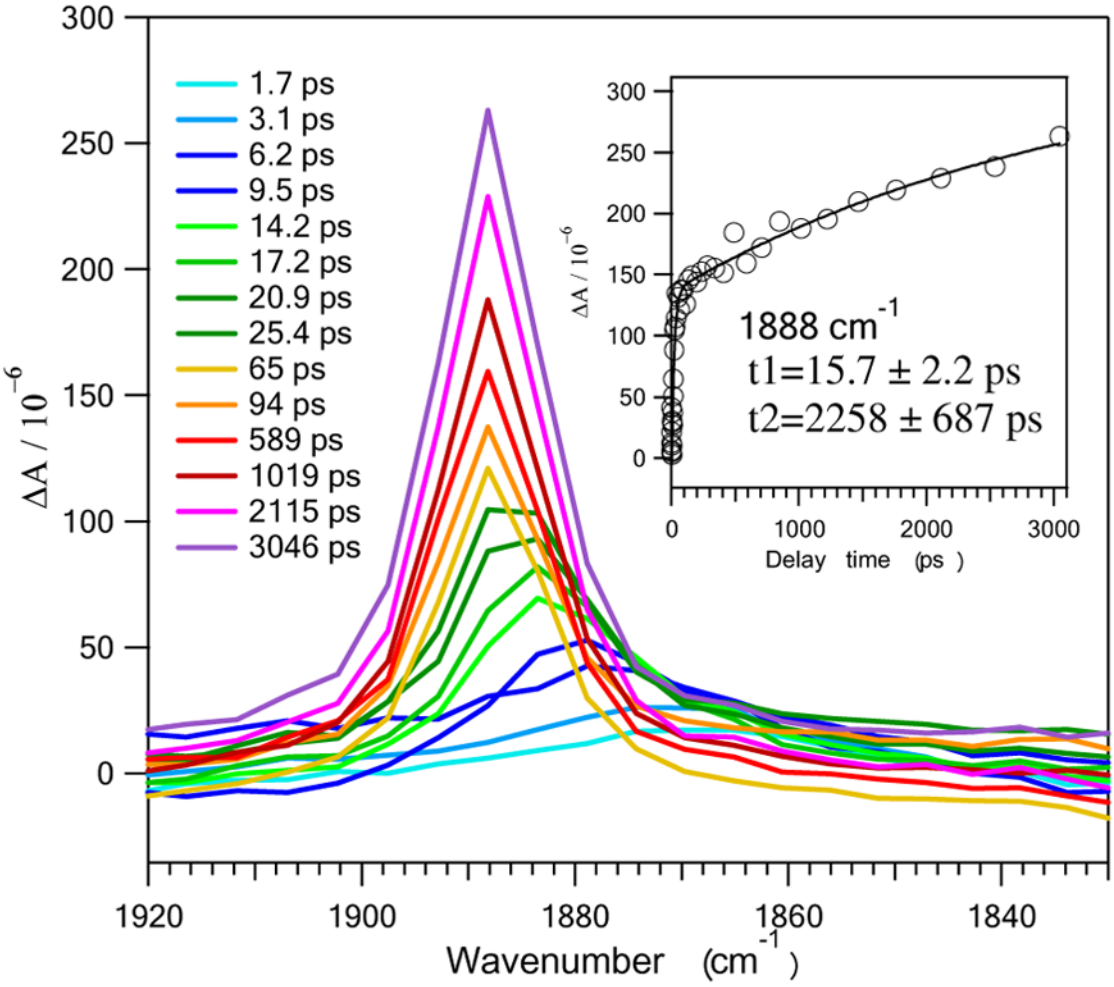

Figure 1.

Transient IR spectra produced after ultrafast photolysis of 4-methoxycarbonylphenyl azide **2a** in MeCN. The spectra were generated by ultrafast LFP (Λ_{ex}=270 nm) and recorded over a time window of 1–3000 ps. (Inset) Kinetic growth at 1888 cm^{-1} as fit by a bi-exponential function.

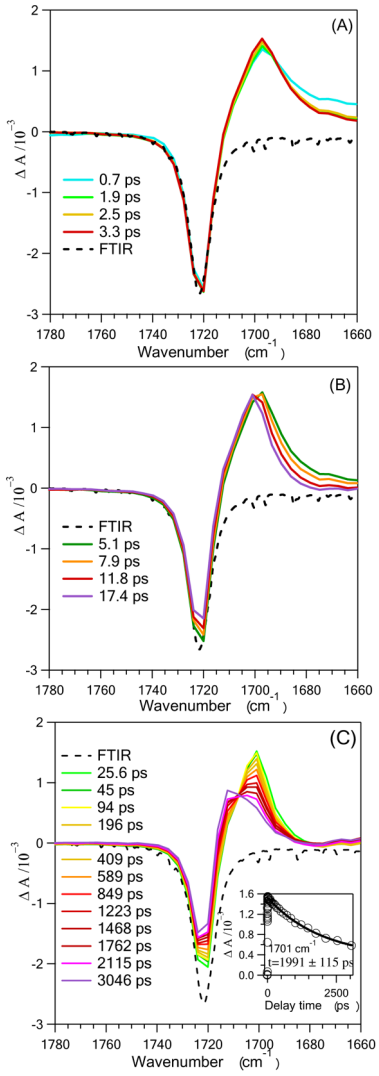

Figure 2.

Transient IR spectra produced after ultrafast photolysis of 4-methoxycarbonylphenyl azide **2a** in MeCN. The spectra were generated by ultrafast LFP (Λ_{ex}=270 nm) recorded over time windows of 0.7–3.3 ps (A), 5.1–17.4 ps (B) and 25.6–3046 ps (C). Kinetic decay at 1701 cm^{-1} as fit by an exponential function (C inset).

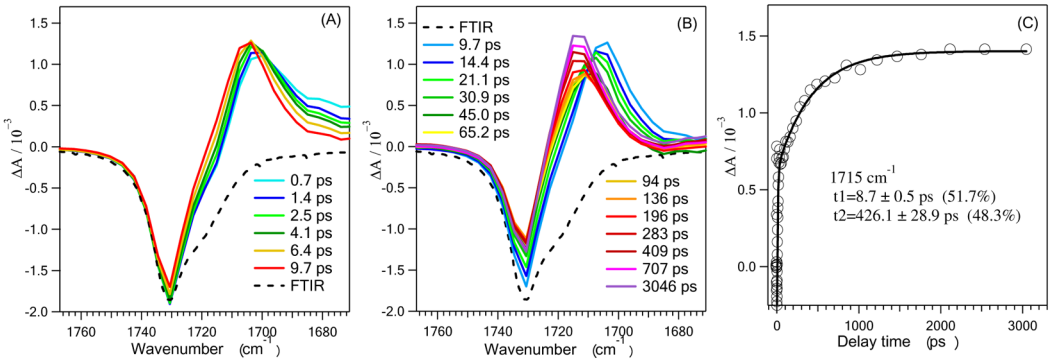

Figure 3.

Transient IR spectra produced after ultrafast photolysis of 2-methoxycarbonylphenyl azide **3a** in MeCN. The spectra were generated by ultrafast LFP (Λ_{ex}=270 nm) over a time window of 0.7–9.7 ps (A), 9.7 ps–3046 ps (B) kinetic growth at 1715 cm^{-1} and fitting with a bi-exponential function (C).

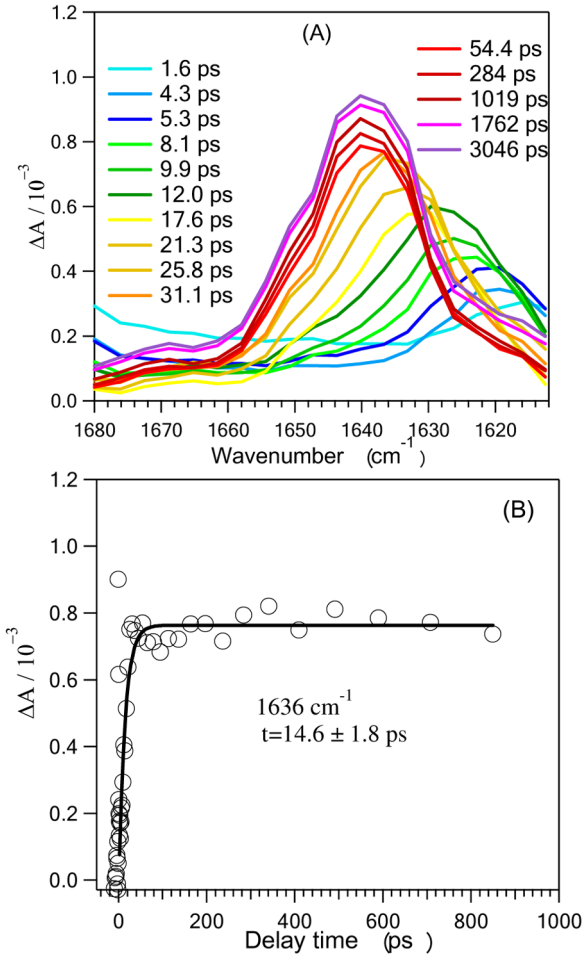

Figure 4.

Transient IR spectra and the kinetics at 1636 cm^{-1} produced after ultrafast 270 nm ultrafast photolysis of 2-methoxycarbonylphenyl azide **3a** in MeCN.

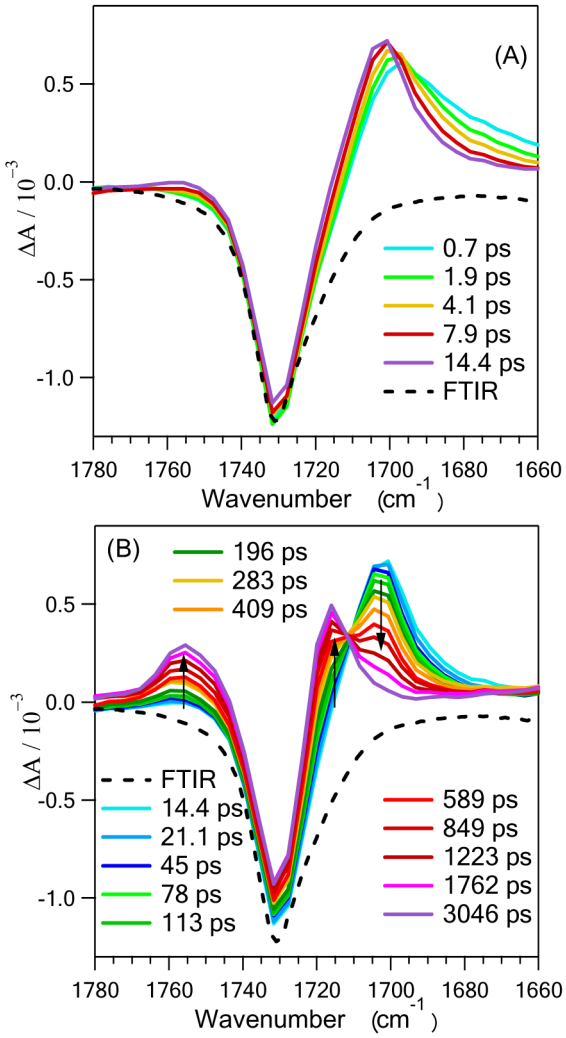

Figure 5.

Transient IR spectra produced after ultrafast photolysis of 2-methoxy-6-methoxycarbonylphenyl azide **4a** in MeCN. The spectra were generated by ultrafast LFP (Λ_{ex}=270 nm) recorded over a time window of 0.7–14.4 ps (A) and 14.4–3046 ps (B).

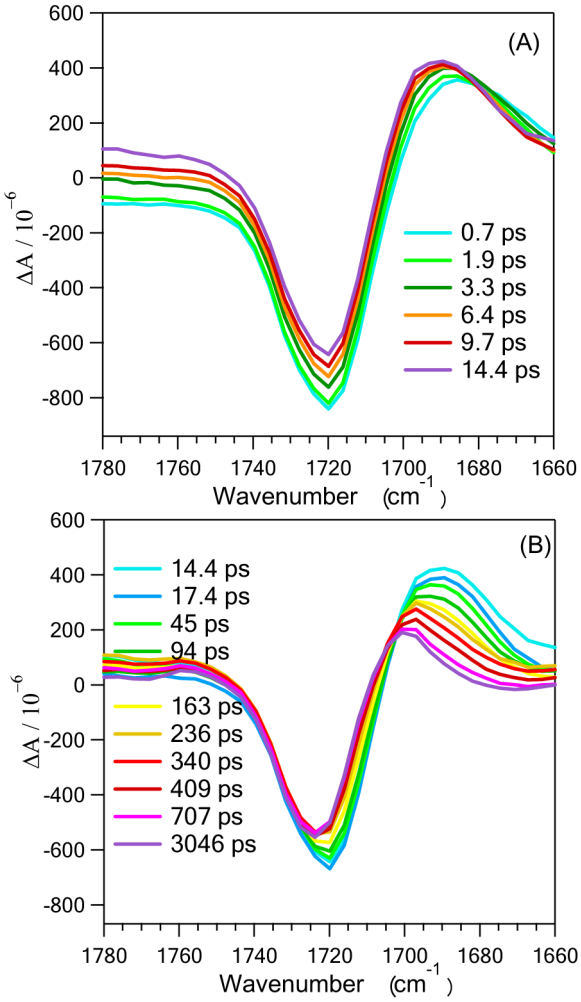

Figure 6.

Transient IR spectra produced after ultrafast photolysis of 2-methoxy-6-methoxycarbonylphenyl azide **4a** in MeCN:D_2O (1:1). The spectra were generated by ultrafast LFP (Λ_{ex}=270 nm,) with a time window of 0.7–14.4 ps (A) and 14.4–3046 ps (B).

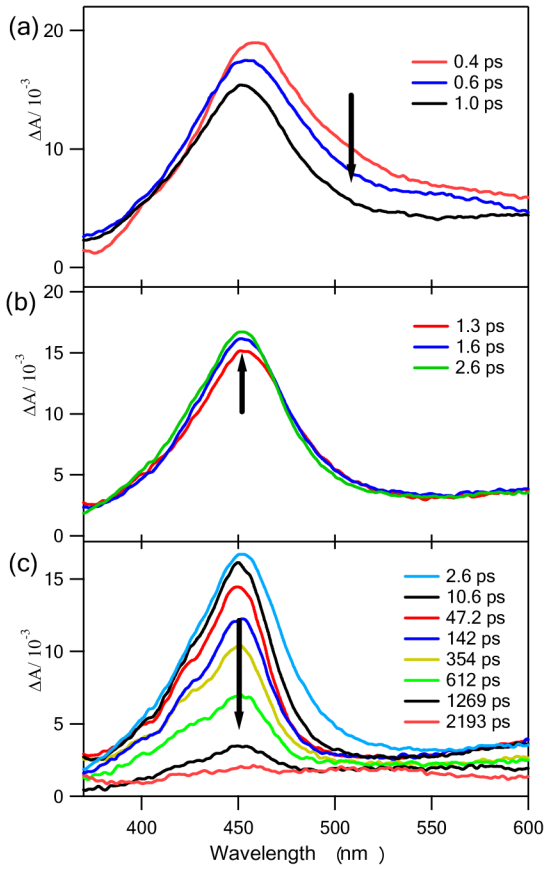

Figure 7.

Transient UV-vis spectra obtained by the photolysis of 2-methoxy-6-methoxycarbonylphenyl azide **4a** in MeCN. Spectra were produced by ultrafast LFP (Λ_{ex}=313 nm) with time window of (a) 0.4–1.0 ps, (b) 1.3–2.6 ps, (c) 10.6–2200 ps.

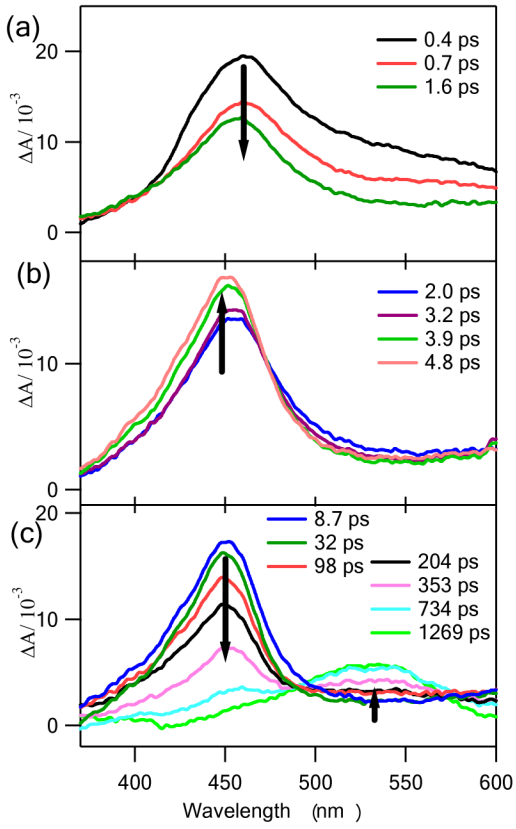

Figure 8.

Transient UV-vis spectra obtained by the photolysis of 2-methoxy-6-methoxycarbonylphenyl azide **4a** in MeCN:H_2O (3:1). Spectra were produced by ultrafast LFP (Λ_{ex}=313 nm) recorded over a time window of (a) 0.4–1.6 ps, (b) 2.0–4.8 ps, (c) 8.7–1200 ps.

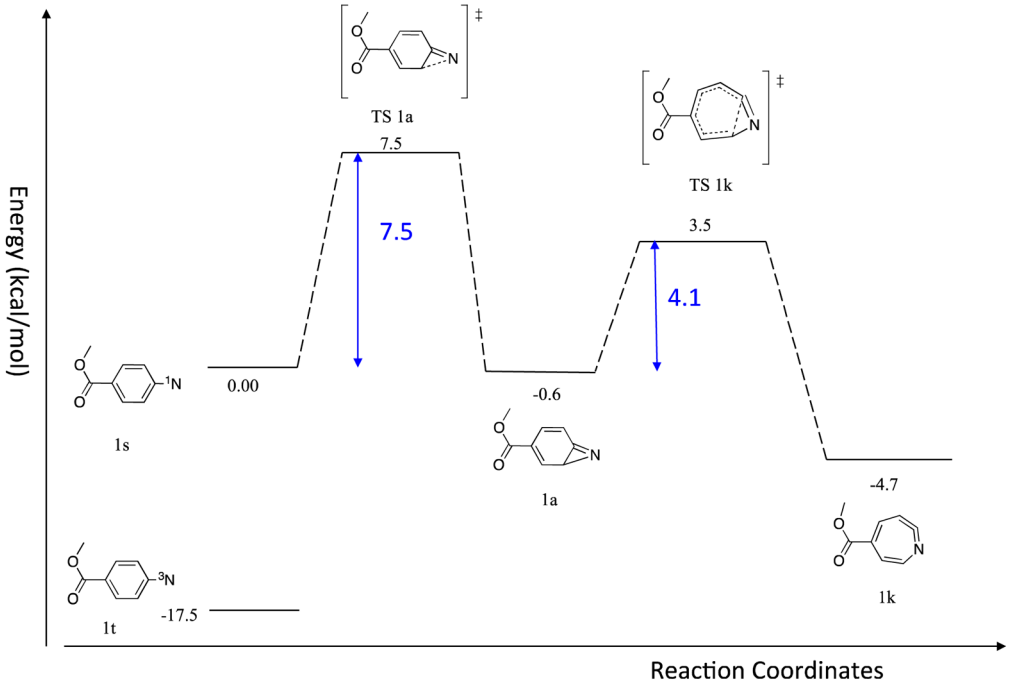

Figure 9.

Relative energy profile (in kcal/mol) obtained from CASPT2/cc-pVDZ//CASSCF(10,10)/6-31G* calculations for ketenimine formation from 4-methoxycarbonylphenylnitrene (**2b** → **2d**).

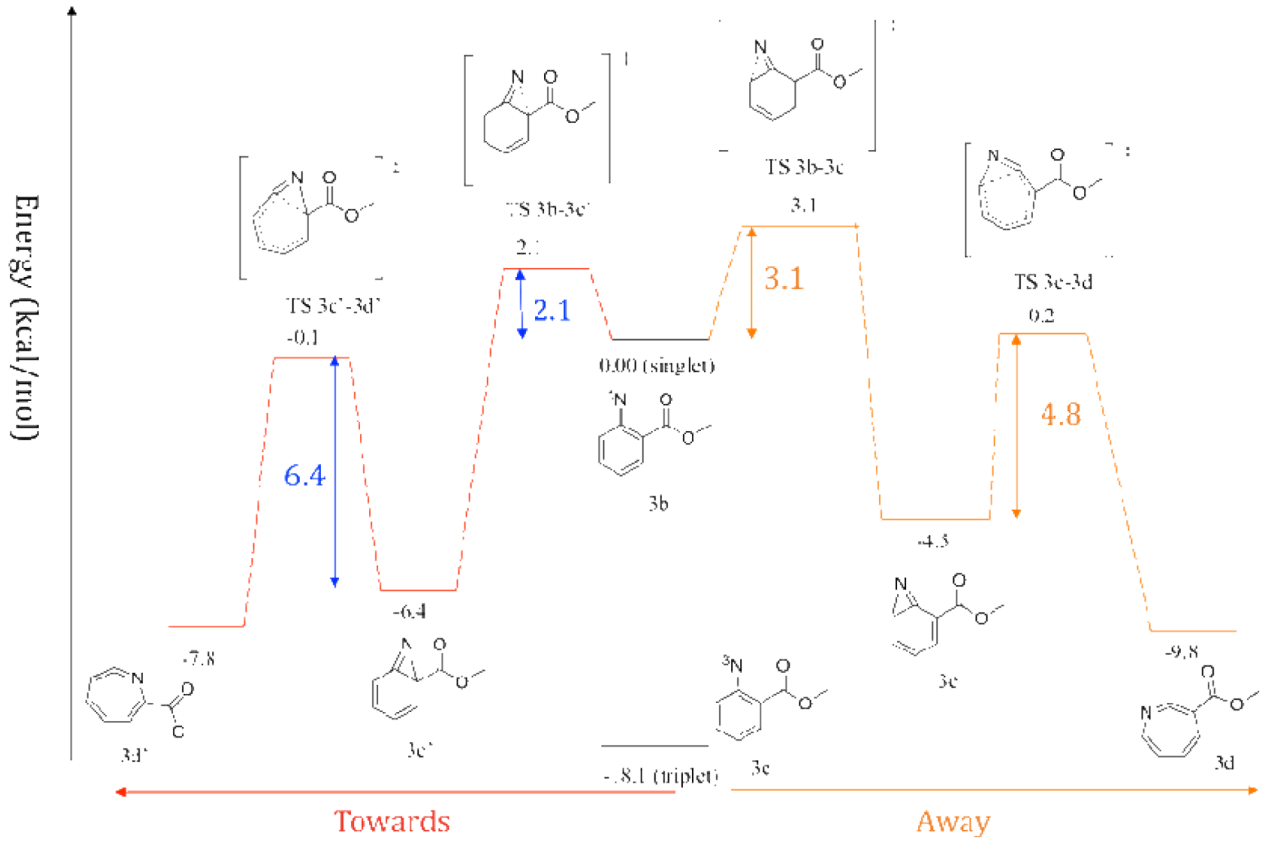

Figure 10.

Relative energy profile (in kcal/mol) obtained from CASPT2/cc-pVDZ//CASSCF(10,10)/6-31G* calculations of ketenimine formation from 2-methoxycarbonylphenylnitrene (**3b** → **3d**).

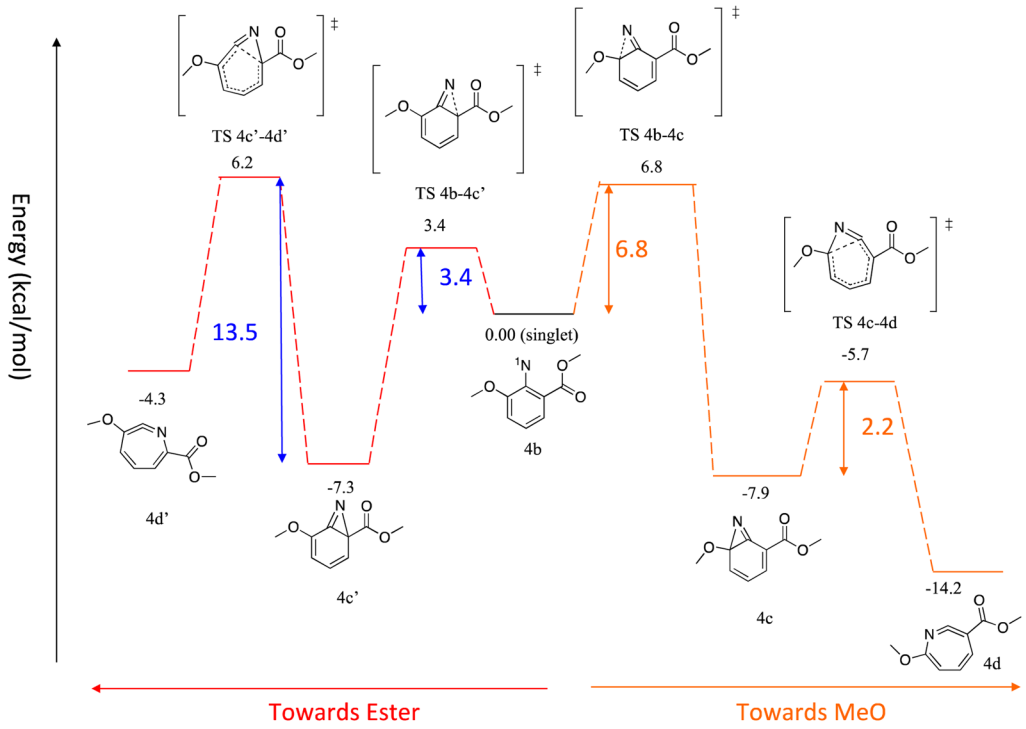

Figure 11.

Relative energy profile (in kcal/mol) obtained for ketenimine formation from 2-methoxy-6-methoxycarbonylphenylnitrene (**4b → 4d**) at the CASPT2/6-31G*//CASSCF(10,10)/6-31G* level of theory.

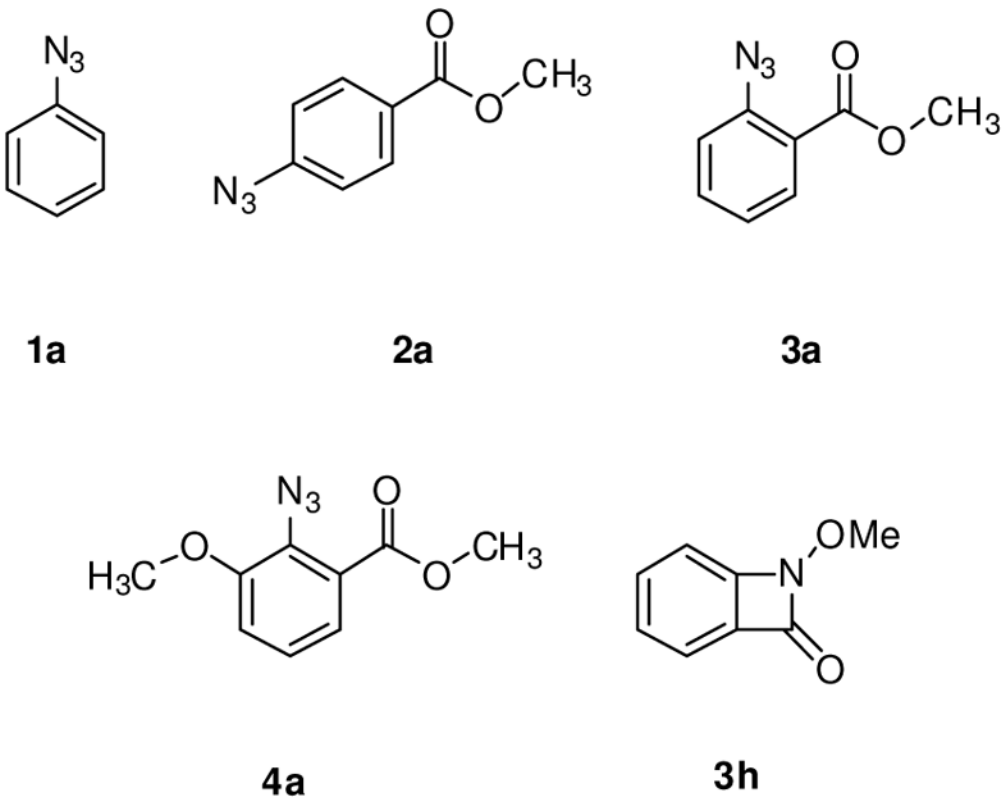

Scheme 1.

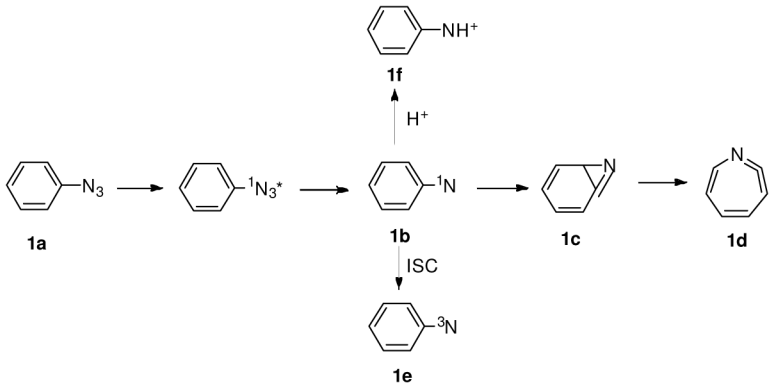

Scheme 2.
The general reaction pathways for arylnitrenes

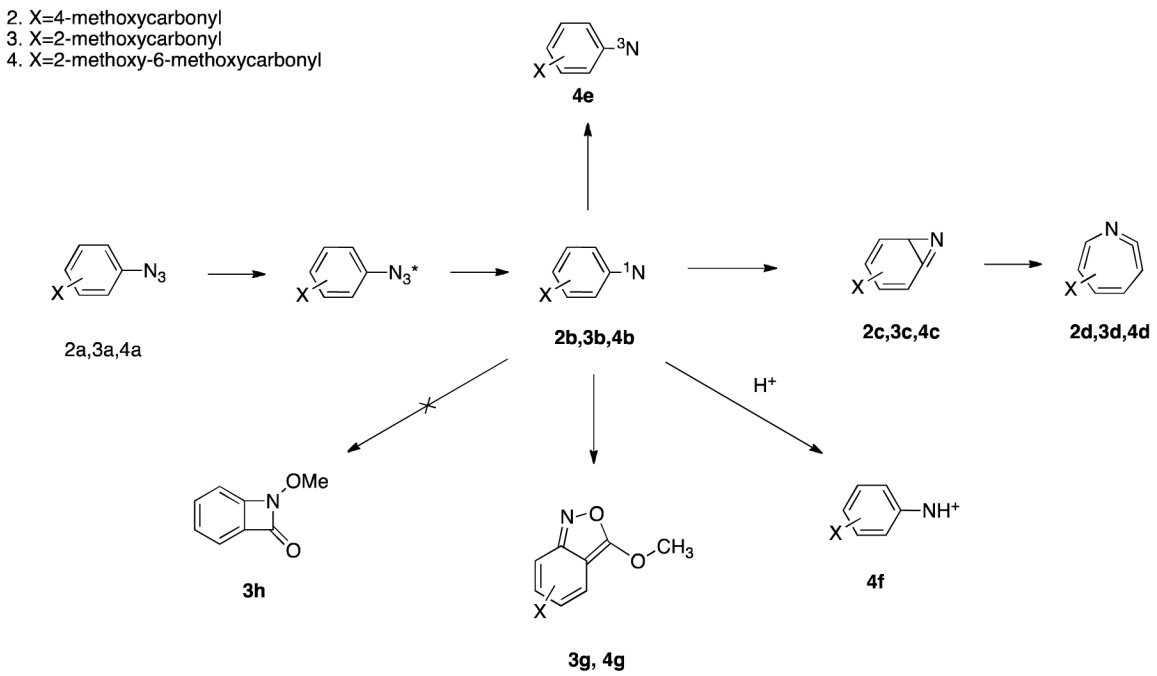

Scheme 3.

Table 1

DFT calculation predicted vibrational frequencies and IR intensities for the MeO-ketenimine and ester-ketenimine (scaling factor: 0.9648).

	Frequencies (cm^{-1})	IR Intensity (KM/mol)	Vibration descriptions
MeO-ketenimine	1866	376	C=C=N stretching
	1705	443	C=O stretching
ester-ketenimine	1862	64	C=C=N stretching
	1703	255	C=O stretching